## An Efficient Design Model for Parallel-guided Layer Jamming Compliant Mechanisms

Xianpai Zeng<sup>1</sup> and Hai-Jun Su<sup>2</sup>

Abstract—Layer jamming (LJ) materials and structures have shown promise in designing variable stiffness compliant mechanisms for robotics. However, design challenges persist due to time-consuming prototyping, testing, and significant computational resources needed for finite element (FE) simulations. The complexity stems from the intricate mechanics behavior between jamming materials and substrate structures. This article presents a hybrid model that combines machine learning (ML) with data generated from finite element (FE) analysis to predict the mechanical behavior of LJ-based compliant parallel-guided mechanisms, including force-deflection relationships, stiffness, and hysteresis. An experimentally validated FE model generates data by varying geometric and material parameters, capturing key mechanical performance metrics. This data serves as input for training a neural network model, which evaluates the impact of selected design parameters on performance metrics. The resulting ML model is highly efficient, with predictions taking seconds compared to hundreds of hours needed for FE simulations, and remarkably accurate, with less than a 5% error relative to FE simulations. This efficient computational model can be used for designing and analyzing LJ-based parallel-guided mechanisms, with the validated workflow process applicable to other LJ-compliant mechanisms and robotic systems.

## I. INTRODUCTION

Layer jamming (LJ) materials and structures have become an attractive solution for stiffness tuning, drawing significant interest in recent years [1]. LJ mechanisms consist of a sealed volume that contains friction layers, with or without a substrate structure. By introducing a pressure differential, the jamming layers are pressed against each other, increasing the friction between them, and significantly enhancing the stiffness of the LJ mechanism. The air pressure can be varied to achieve a continuum of stiffness values. Wall et al. [2] demonstrated that LJ has the highest range of stiffness or stiffness change ratio among the three jamming methods (LJ, grain, and fiber). Furthermore, the force-deflection behavior comparison presented in [3] indicates the superiority of LJ over other jamming mechanisms under bending load. LJ has been successfully applied in various robotic devices, including variable stiffness mechanisms [4] and high-performance variable stiffness robotic grippers [5], [6], [7].

The ability of LJ structures to vary stiffness with minimal mechanical design overhead makes them ideal candidates for designing mechanisms and robotic devices, such as soft grippers, with enhanced payload capacity [8], [9], [10]. To handle

delicate objects or work alongside human operators, robots require both flexibility and rigidity [11], [12]. Robots capable of controlling their stiffness can significantly enhance their load carrying capability while maintaining flexibility when not carrying a load. For instance, a robot capable of varying its stiffness can become more rigid when load capability is needed, but can also become more compliant to avoid injuring surrounding humans or damaging the load. Kim et al. [13], [14] developed a manipulator using LJ for minimally invasive surgery that can assume a flexible state for insertion without accidental injury, but can then become stiff to achieve the required positional accuracy. This marks the beginning of exploring the application of LJ as an effective variable stiffness solution. Recent studies and applications of LJ mechanisms have focused on finding new designs of backbones on which jamming layers are attached [15], [16] or exploring appropriate application scenarios [17], [18], [19], [20], [21], [22].

Design modeling of LJ mechanisms remains a significant challenge due to the complexity of the underlying mechanics of these materials and structures. Several mechanics models have been developed to quantify the relationship between performance metrics and design parameters [23], [24], [25]. Finite Element models have also been developed to simulate the mechanics behavior of LJ structures [26] and have shown great accuracy compared with experimental tests. However, the FE model developed in the study only demonstrates force-deflection behavior and does not offer the capability of sizing design parameters for performance metrics. This capability, often called the "inverse design model," has not been comprehensively addressed in LJ literature. Zeng et al. [27] proposed a preliminary inverse design model based on a mechanics mode for an LJ-based parallel-guided compliant mechanism. However, due to the large number of frictional contact pairs, large deflection, and non-linear nature, these FEA simulations are computationally expensive, taking 20-40 hours each. Thus, generating the entire solution space efficiently is impossible [27].

In the aerospace industry, researchers have used numerical optimization to generate optimum aerodynamic shapes, substantially reducing experimental time and costs [28]. A comparable computational methodology is needed for the design of robotic jamming layer structures to reduce the design cycle. Specifically, a highly efficient and accurate computational tool is needed to (1) predict a design's performance prior to prototyping, and (2) determine design parameters to meet predefined performance metrics.

 $<sup>^1\</sup>rm{Xianpai}$  Zeng is with Research and Development, FANUC America Corporation, Rocheser Hills, Michigan, 48309, USA Xianpai.Zeng@fanucamerica.com

<sup>&</sup>lt;sup>2</sup>Hai-Jun Su is with Faculty of the Department of Mechanical and Aerospace Engineering, The Ohio State University, Columbus, Ohio 43210, USA su.298@osu.edu

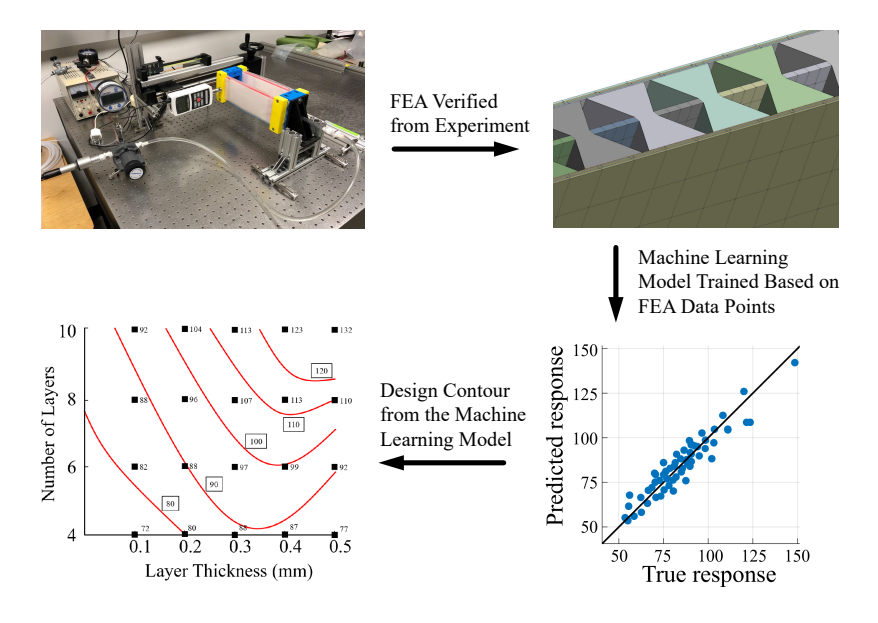


Fig. 1: The work flow to train and apply the machine learning model for performance prediction of LJ mechanisms.

## II. WORK FLOW OF THE MACHINE LEARNING MODEL

The finite element simulation of LJ mechanisms is extremely computationally expensive, taking tens of hours, making it highly inefficient. To overcome this challenge, we propose a machine learning (ML) model for predicting the performance of LJ-based compliant mechanisms. To demonstrate the process, we use the compliant parallel-guided mechanism shown in Figure 1. The goal is to explore the entire design space of this type of mechanism and develop a highly efficient model to gain deeper insights into how key performance metrics are determined by various design/control parameters.

Figure 1 illustrates the basic workflow for training the ML model and applying it to performance prediction. The first step is to develop an accurate finite element (FE) model for evaluating the key performance metrics. The second step involves running numerous FEA simulations by sweeping geometric/material/control parameters to identify the key performance metrics, including the stiffness change ratio, maximum achievable stiffness, and residue deflection, among others. Although this step is the most time-consuming (taking hundreds of simulation hours), it is a one-time computation. In the third step, we feed the simulation data to a neural network model that maps the performance metrics to the design parameters. The trained model is highly efficient and capable of predicting the performance metrics based on the input of design parameters in seconds rather than hours. We can then use this ML model to generate the entire design space by sampling the design and control parameters. The result is a novel, efficient, and accurate computational model that can be used for the design and analysis of LJ compliant mechanisms in the early design iterations.

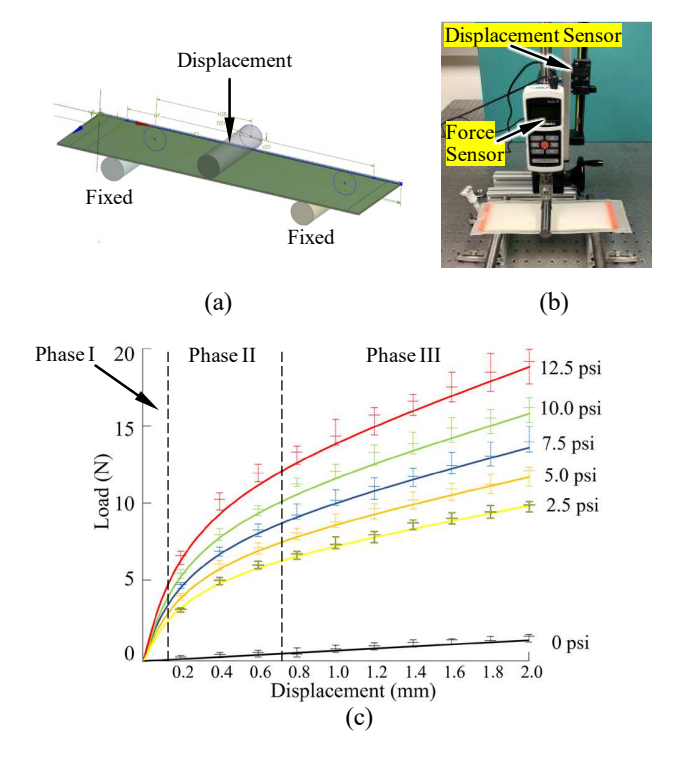


Fig. 2: Initial FE model calibration based on a stack of layers under 3-point bending. (a) FE model of a stack of layers. (b) Experiment setup. (c) FE data compared with experiment result. The vertical bars are experimental testing data. And the curves are the FE simulation data.

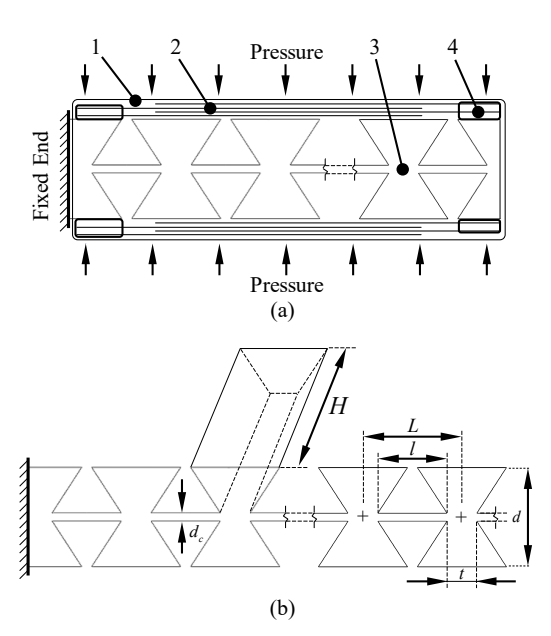


Fig. 3: The parallel-guided LJ mechanism. (a): Main components of the parallel-guided compliant mechanism showing (1) Vacuum Membrane, (2) Jamming Layers, (3) Hourglass Shaped Beam (Substrate), (4) Layer Clamp. (b): The geometric design parameters of a single beam.

#### III. CALIBRATION OF THE MATERIAL PROPERTIES

To develop a finite element model of an LJ compliant mechanism, we must first calibrate the material properties to match the FE model with experimental results. To do so, we develop a FE model for a stack of jamming layers and calibrate the material properties by comparing the results with physical experiments as shown in Fig. 2. The jamming layers are made from polyester film, which typically has a modulus of elasticity ranging from 3.10 GPa to 4.36 GPa. Meanwhile, the vacuum membrane is made of Polyurethane elastomer, which has a wide range of modulus of elasticity from 0.00114 GPa to 0.248 GPa (Matweb). The modulus of the polyester film is iterated from 3.10 GPa to 4.4 GPa with an increment of 0.10 GPa, while the modulus of the Polyurethane elastomer is iterated from 0.005 GPa to 0.25 GPa with an increment of 0.005 GPa. The calibrated material parameters are listed in Table I, with the friction coefficient obtained from a previous study using the same materials [27]. The modulus of elasticity of the beam material is also obtained from this study.

# IV. THE PARALLEL GUIDED LAYER JAMMING MECHANISM

## A. The finite element model

For more details on the parallel-guided compliant mechanism, please refer to the work of Zeng et al [4].

The finite element model configuration, presented in Fig.4 (a), comprises hour-glass shaped sections that are relatively more rigid compared to the thin beam sections. Since the

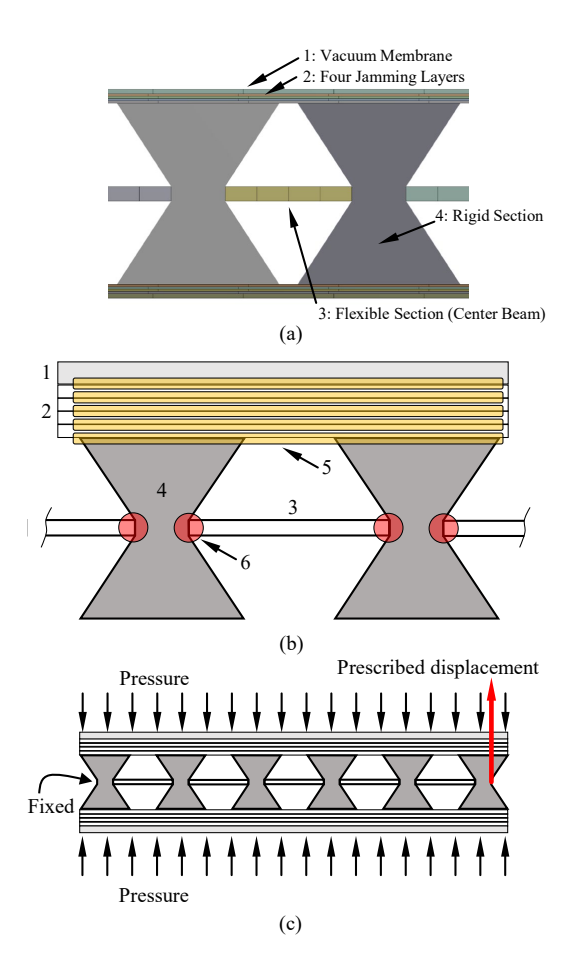


Fig. 4: The finite element model. (a) FEA configuration showing the major components: 1. Vacuum Membrane. 2. Jamming Layers. 3. Flexible Section of the Beam (Center Beam). 4. Rigid Section of the Beam (Hourglass-Shaped Structure). (b) FEA schematic figure showing the contact pairs: 5. Frictional Contact Pairs. 6. Rigid Connections. (c) Boundary conditions.

more rigid hour-glass sections exhibit significantly lower stress and deflection, the primary interest lies in calculating the stress and deformation in the thin beam sections. Therefore, all the hour-glass shaped sections are defined to have a rigid stiffness behavior. To model the frictional contact pairs between the beam and bottom jamming layer, in-between jamming layers, and between the top jamming layer and vacuum bag, a coefficient of friction of 0.167 is used based on experimental measurements of the jamming layers. The contact formulation uses augmented Lagrange to achieve minimal penetration, high robustness, and low computational cost. Table I lists the dimensions and material properties used in the model.

## B. Sensitivity Analysis of Key Design Parameters

The geometric and material design parameters of the compliant parallel-guided mechanism are presented in Table I and illustrated in Fig. 3 (b). The geometric parameters consist of the number of jamming layers N, the beam

TABLE I: The design parameters for the FE model

Symbol	mbol Description									
Key Design Parameters										
N	number of frictional layers on each side	4								
H	beam height	$75\mathrm{mm}$								
d	beam thickness	$10\mathrm{mm}$								
$d_c$	center beam thickness	$0.8\mathrm{mm}$								
Material Parameters										
$E_l$	modulus of layer material	$4.0\mathrm{GPa}$								
$E_b$	modulus of beam material	$2.6\mathrm{GPa}$								
$E_v$	modulus of vacuum membrane material	$0.02\mathrm{GPa}$								
$\mu$	friction coefficient	0.167								
Beam Dimensions										
$L_b$	beam length	$227\mathrm{mm}$								
l	length of flexible part of one unit	$7\mathrm{mm}$								
t	length of rigid part of one unit	$3\mathrm{mm}$								
L	total length of one unit	$10\mathrm{mm}$								
n	total number of unit sections	23								

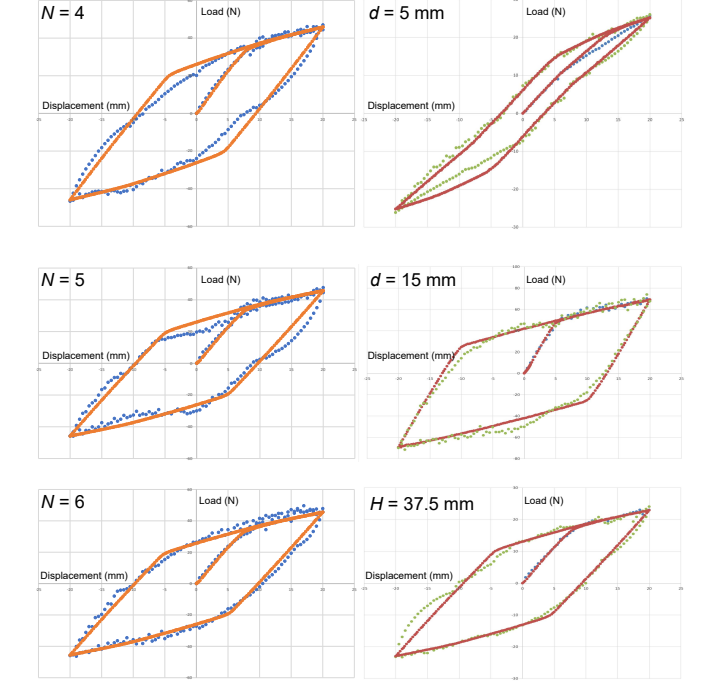


Fig. 5: Comparison of the experimental results and the finite element simulations. The dots represent the experimental data while the curves represent the simulation data.

thickness d, the center beam thickness dc, and the beam height H, while the material parameters include the elastic modulus of the beam material Eb and the elastic modulus of the layer material  $E_l$ .

To verify the finite element (FE) model employed in the parallel-guided mechanism, experiments were carried out with varying design parameters, including the number of layers, beam thickness, and beam height. The respective experimental and FE results were gathered and compared in Fig.5. Both the experimental and FE studies obtained the full loading and unloading curves to exhibit the hysteresis behavior of the jamming structures.

With the FE model validated by experimental results, a thorough sensitivity analysis is conducted by varying all the geometric and material design parameters. Each design parameter is increased and decreased by 25% and 50%, respectively, to investigate its effect on the system's behavior. All the design studies are listed in Fig. 6. A design principle for achieving a higher stiffness ratio in the parallel-guided mechanism can be drawn from these studies.

- 1) Estimated from the spacing between the curves, the parameters that exhibit the highest sensitivity to stiffness ratio are the beam height (H), beam thickness (d), and center beam thickness  $(d_c)$ .
- A higher modulus of the layer material results in a greater stiffness ratio. This can be attributed to the higher stiffness achieved due to the increased modulus of the layer material.
- 3) Increasing the number of layers leads to a higher stiffness ratio, but its effect is not as significant as that of varying H, d, or  $d_c$ .
- 4) Both the beam height and the center beam thickness are negatively correlated with the stiffness ratio. A decrease in these parameters can lead to a higher stiffness ratio; however, this may result in a greater maximum stress, which can compromise the loadcarrying capacity of the design. Thus, it is necessary to exercise caution when reducing the beam height and center beam thickness.

## V. DEVELOPMENT OF THE MACHINE LEARNING MODEL

The compliant parallel-guided mechanism with LJ has eight key design parameters, including beam height, beam thickness, center beam thickness, number of layers, modulus of elasticity of the beam material, modulus of elasticity of the layer material, layer thickness, and the ratio of modulus of elasticity of layer and beam materials. However, each curve in Fig.6 only corresponds to one design point in the design space and takes about 10-30 hours to compute. As a result, it would be computationally expensive to generate a comprehensive design contour that could indicate the trend of stiffness ratio or other performance metrics with continuously changing design parameters.

Five groups of two design parameters were selected, as shown by the black squares in Fig.7. A total of 86 FEA studies were carried out using the uniformly selected parameter pairs in these five sub-design spaces. A ML model was then built based on the 86 sets of design parameters and the stiffness ratio change. The small dataset was less likely to suffer from the over-fitting problem. Hyper-parameters were tuned to avoid overfitting as well as to achieve high accuracy. The hyper-parameters of the narrow neural network are listed in Table II. Design contour curves were plotted on top of the FEA design points, facilitating the comprehension of the stiffness ratio change corresponding to a design parameter variation.

In addition to the stiffness ratio, the maximum stiffness achievable by the layer jamming mechanism is also a significant parameter, as it is directly related to the load capacity. To

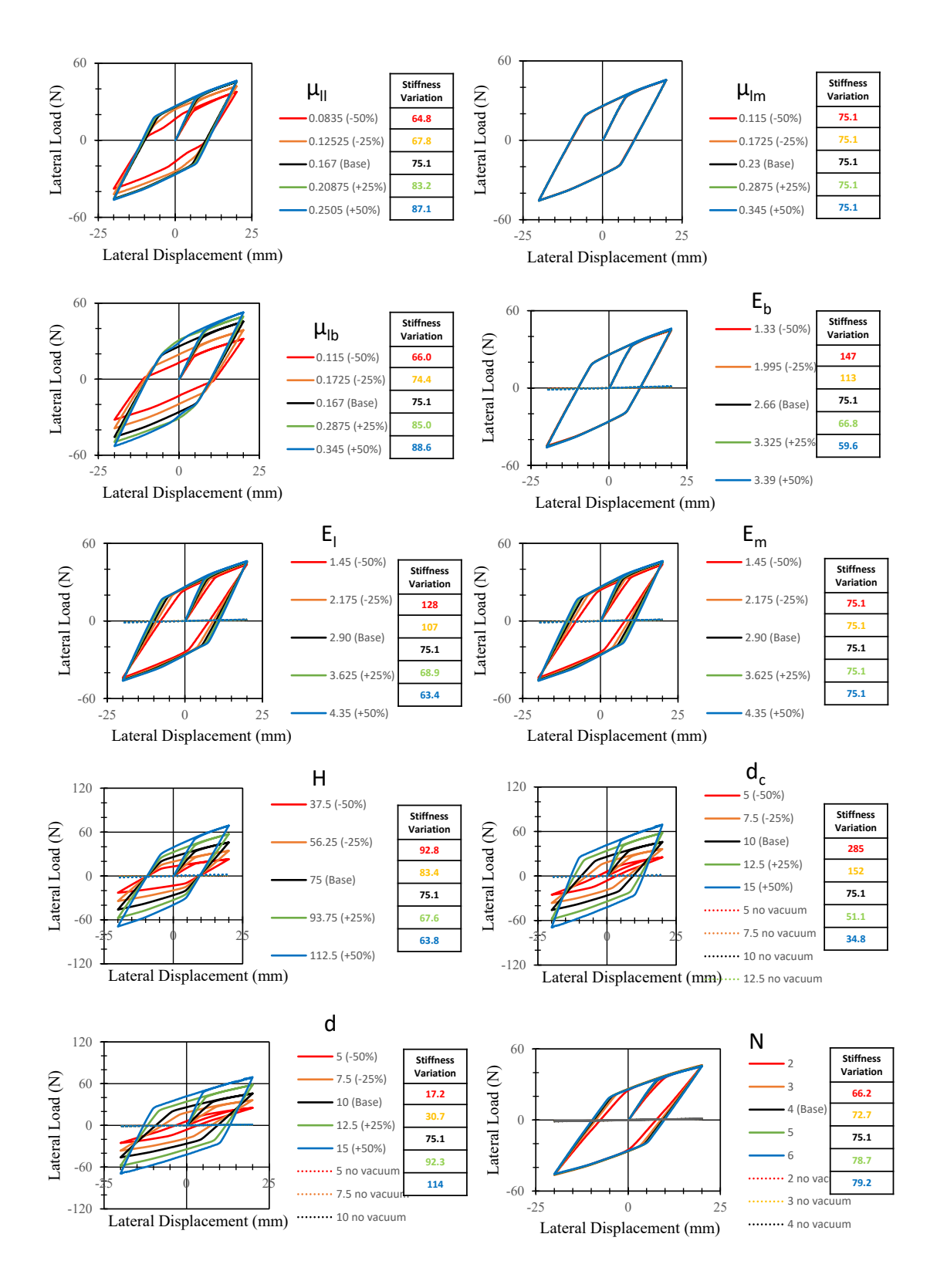


Fig. 6: Sensitivity Analysis on Key Design Parameters Based on the ML model.

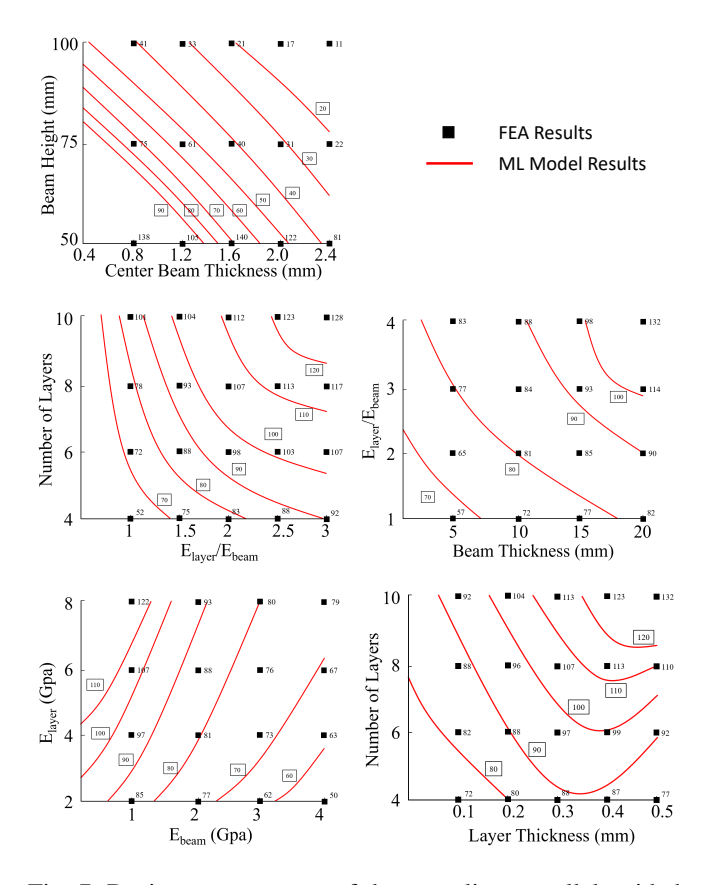


Fig. 7: Design contour map of the compliant parallel-guided mechanism with layer jammming.

explore the design space for maximum stiffness, a separate set of FEA simulations was conducted and a machine learning model was trained on this design space. The resulting sensitivity studies are presented in Fig. 8, which clearly indicate that the beam height H and beam thickness d are the most sensitive design parameters for maximum stiffness, while the modulus of elasticity of the beam material  $E_b$  is the least sensitive. This finding is consistent with the fact that the maximum stiffness is primarily influenced by the jammed layer, which is mainly affected by the modulus of the layer material.

- F<sub>max-preslip</sub> is the maximum load the mechanism can bear before the mechanism starts to have excessive deformation caused by the slip within jamming layers. The beam thickness, d, and the beam height, H, are the two parameters that contribute most to a high load capacity.
- 2)  $d_{res}$  is the residue deformation when the beam is unloaded by removing the external load. It characterizes the hysteresis caused by the friction forces between the jamming layers. The study suggests that lower beam thickness, d, and lower modulus of elasticity of the layer material,  $E_l$ , would lead to a low hysteresis design. Fewer number of jamming layers, N, would also help to reduce hysteresis, not as effectively as the aforementioned parameters though.

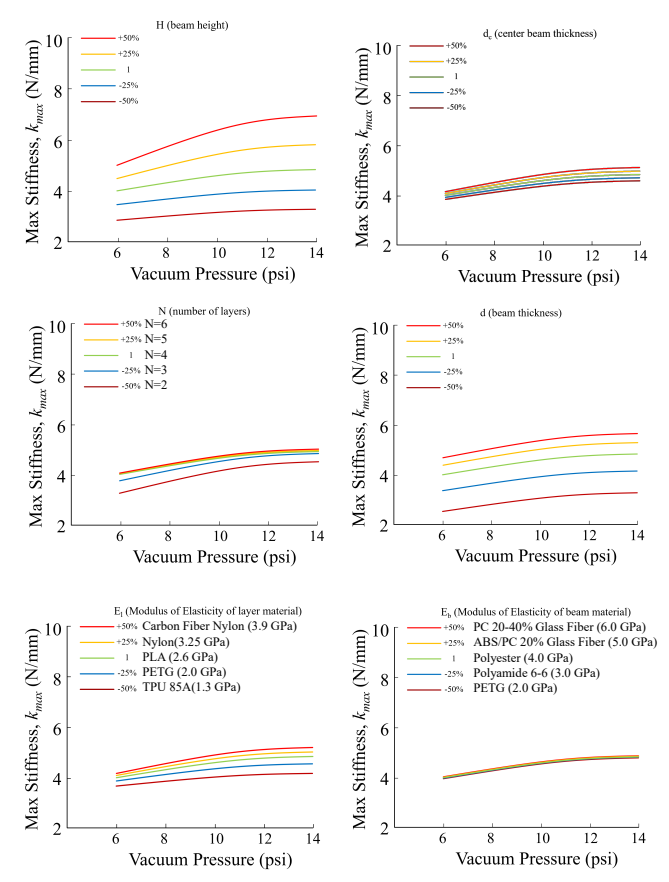


Fig. 8: Max stiffness vs. design parameters

3) Maximum stiffness,  $k_{max}$ , is desired for high precision on motion and manipulation. The study shows that higher beam thickness, d, and higher modulus of elasticity of the layer material,  $E_l$ , would give a higher maximum stiffness.

The studies presented in Fig. 9 suggest that the most sensitive design parameters can be manipulated to achieve a specific performance metric. However, modifying design parameters to optimize one performance metric may have an adverse effect on another metric. For example, increasing the beam thickness, d, and the modulus of elasticity of the layer material,  $E_l$ , may result in a higher maximum stiffness, but it may also cause higher hysteresis.

To assess the accuracy of the machine learning models built from FEA studies, 10 sets of randomly selected design parameters were chosen, and performance metrics were calculated using both the machine learning model and the FEA model. In Table III, the results were compared, and it was found that the largest deviation from the machine learning model results to the FEA results was within 5%.

## VI. CONCLUSIONS

In this article, a machine learning model was developed and trained on the finite element studies to predict the mechanics behavior of a layer jamming based compliant parallel-guided mechanism, including force-deflection relation, maximum achievable stiffness, and hysteresis. The traditional method of swiping input parameters to generate the design space is inefficient due to the high computational cost caused by the complicated mechanical interactions of the jamming layers. The machine learning model was trained using the data generated from the finite element model, which was experimentally validated. The ML model has a comparable accuracy (5% error) with the finite element model but takes only seconds to achieve the prediction, compared to the several hundreds of hours needed for the finite element model.

Due to the high computational cost of finite element analysis, the number of evaluations is severely limited. To overcome this challenge, a fast machine learning model was trained based on the finite element studies. This model predicts the effects of selected key design parameters on the mechanics behaviors, providing guidelines for the optimal design of layer jamming mechanisms for a selected performance metric. The trend on which the performance metrics vary with the design parameters can be used in the preliminary design stage of layer jamming mechanisms to provide initial design decisions regarding dimensions and material selections.

## VII. ACKNOWLEDGMENT

This material is based upon work supported by the National Science Foundation under Grant No. 2019648. Any opinions, findings, and conclusions or recommendations expressed in this material are those of the author(s) and do not necessarily reflect the views of the funding agencies.

#### REFERENCES

- [1] Ou, J., Yao, L., Tauber, D., Steimle, J., Niiyama, R., and Ishii, H., 2013. "jamSheets: thin interfaces with tunable stiffness enabled by layer jamming". In Proceedings of the 8th International Conference on Tangible, Embedded and Embodied Interaction TEI '14, ACM Press, pp. 65–72.
- [2] Wall, V., Deimel, R., and Brock, O., 2015. "Selective stiffening of soft actuators based on jamming". In 2015 IEEE International Conference on Robotics and Automation (ICRA), pp. 252–257.

TABLE II: The hyper-parameters of the narrow neural network

Narrow Naural Natwork Hypernarameters

Narrow Neural Network Hyperparameters							
Hyperparameter	Value						
Number of fully connected layers	3						
Size of each fully connected layer	60, 50, 40						
Activation	ReLU (Rectified Linear Unit)						
Iteration limit	100						
Regularization term strength	0						
Standardize data	Yes						

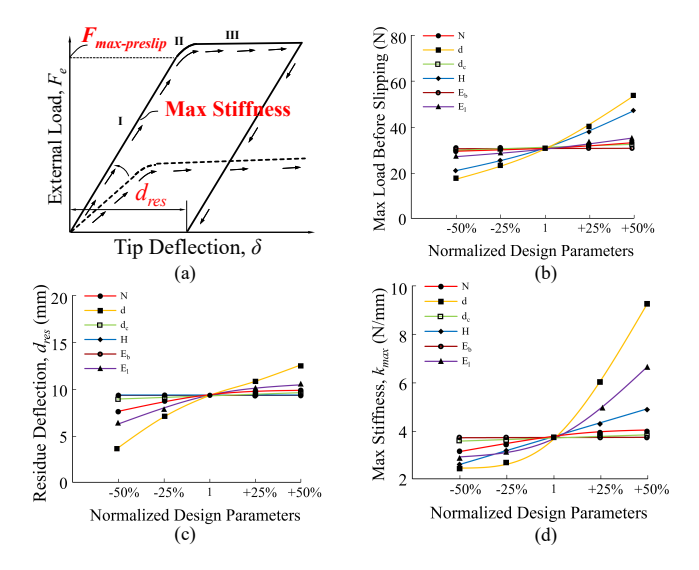


Fig. 9: Performance Metrics ( $F_{max-preslip}$ ,  $d_{res}$ ,  $k_{max}$ ) vs. Design Parameters. (a) The figure defines three metrics including  $F_{max-preslip}$ ,  $d_{res}$ , and  $k_{max}$ . (b)  $F_{max-preslip}$  is the maximum load the mechanism can bear before the mechanism starts to have excessive deformation caused by the slip within jamming layers. (c)  $d_{res}$  is the residue deformation when the beam is unloaded by removing the external load. It characterizes the hysteresis caused by the friction forces between the jamming layers. (d) Maximum stiffness,  $k_{max}$ , is desired for high precision on motion and manipulation.

- [3] Aktaş, B., Narang, Y. S., Vasios, N., Bertoldi, K., and Howe, R. D., 2021. "A Modeling Framework for Jamming Structures". Adv. Funct. Mater., 31(16), Apr., p. 2007554.
- [4] Zeng, X., Hurd, C., Su, H.-J., Song, S., and Wang, J., 2020. "A parallel-guided compliant mechanism with variable stiffness based on layer jamming". *Mechanism and Machine Theory*, 148, June, p. 103791.
- [5] Gao, Y., Huang, X., Mann, I. S., and Su, H.-J., 2020. "A Novel Variable Stiffness Compliant Robotic Gripper Based on Layer Jamming". *Journal of Mechanisms and Robotics*, 12(5), Oct., p. 051013.
- [6] Crowley, G. B., Zeng, X., and Su, H.-J., 2022. "A 3D Printed Soft Robotic Gripper With a Variable Stiffness Enabled by a Novel Positive Pressure Layer Jamming Technology". *IEEE Robotics and Automation Letters*, 7(2), Apr., pp. 5477–5482.
- [7] Zeng, X., and Su, H.-J., 2023. "A High Performance Pneumatically Actuated Soft Gripper Based on Layer Jamming". *Journal of Mechanisms and Robotics*, 15(1), Feb., p. 014501.
- [8] Yang, Y., Zhang, Y., Kan, Z., Zeng, J., and Wang, M. Y., 2020. "Hybrid Jamming for Bioinspired Soft Robotic Fingers". Soft Robotics, 7(3), June, pp. 292–308.
- [9] Wang, X., Wu, L., Fang, B., Xu, X., Huang, H., and Sun, F., 2020. "Layer jamming-based soft robotic hand with variable stiffness for compliant and effective grasping". *Cognitive Computation and Systems*, 2(2), June, pp. 44–49.
- [10] Fang, B., Sun, F., Wu, L., Liu, F., Wang, X., Huang, H., Huang, W., Liu, H., and Wen, L., 2021. "Multimode Grasping Soft Gripper Achieved by Layer Jamming Structure and Tendon-Driven Mechanism". Soft Robotics, June, p. soro.2020.0065.
- [11] Rus, D., and Tolley, M. T., 2015. "Design, fabrication and control of soft robots". *Nature*, 521(7553), May, pp. 467–475.
- [12] Trivedi, D., Rahn, C. D., Kier, W. M., and Walker, I. D., 2008. "Soft robotics: Biological inspiration, state of the art, and future research". *Applied Bionics and Biomechanics*, 5(3), Dec., pp. 99–117.
- [13] Kim, Y.-J., Cheng, S., Kim, S., and Iagnemma, K., 2012. "Design of a tubular snake-like manipulator with stiffening capability by layer

TABLE III: Machine Learning Model Accuracy Verification

Design Parameters					Stiffness Ratio			Max Stiffness (N/mm)		Max Load before Slip (N)			Residual Deflection (mm)				
N	d (mm)	dc (mm)	H (mm)	Eb (GPa)	El (GPa)	FEA	ML	Error	FEA	ML	Error	FEA	ML	Error	FEA	ML	Error
7	5	1.2	71	4	6	61.1	58.7	-4.12%	2.6	2.7	3.40%	22.8	22.7	-0.25%	3.2	3.1	-4.30%
7	7	1.6	68	3	4.3	75.7	79.4	4.67%	2.8	2.9	3.27%	25.8	25.2	-2.25%	5.5	5.8	4.46%
6	5	1.1	87	3	3.5	62.2	64.1	2.95%	2.6	2.5	-4.95%	21.4	20.8	-2.87%	4.4	4.5	2.86%
1	6	1	81	2.7	3	66.7	65.7	-1.48%	3	3.0	-0.13%	26.5	27.2	2.62%	4.7	4.6	-1.51%
2	14	1.3	65	2.7	4.8	77.8	75.7	-2.84%	6.1	6.2	1.85%	57.2	58.4	2.08%	12.1	11.8	-2.92%
1	11	1.4	83	2.2	2.7	72.7	74.2	2.03%	5.7	5.7	0.32%	32.4	32.5	0.37%	11.5	11.7	1.99%
5	5	0.9	61	3.8	5.2	71.5	74.8	4.39%	2.5	2.5	1.58%	22.6	21.6	-4.60%	4.5	4.7	4.20%
5	5	1.2	80	2.4	5.2	65.3	62.6	-4.26%	2.3	2.3	0.41%	24.2	24.4	0.73%	4.7	4.5	-4.45%
1	10	1.8	73	3.7	2.3	72.3	70.0	-3.26%	4.1	4.2	2.08%	31.1	32.1	3.22%	9.1	8.8	-3.37%
8	5	0.9	80	3.5	4.2	70.4	67.9	-3.70%	2.6	2.5	-2.55%	26.8	26.5	-1.15%	4.8	4.6	-3.84%

- jamming". In 2012 IEEE/RSJ International Conference on Intelligent Robots and Systems, IEEE, pp. 4251–4256.
- [14] Kim, Y., Cheng, S., Kim, S., and Iagnemma, K., 2013. "A Novel Layer Jamming Mechanism With Tunable Stiffness Capability for Minimally Invasive Surgery". *IEEE Transactions on Robotics*, 29(4), Aug., pp. 1031–1042.
- [15] Santiago, J. L. C., Godage, I. S., and Walker, I. D. "Soft Robots and Kangaroo Tails: Modulating Compliance in Continuum Structures via Mechanical Layer Jamming". p. 18.
- [16] Deshpande, A. R., Tse, Z. T. H., and Ren, H., 2017. "Origami-inspired bi-directional soft pneumatic actuator with integrated variable stiffness mechanism". In 2017 18th International Conference on Advanced Robotics (ICAR), IEEE, pp. 417–421.
- [17] Simon, T. M., Thomas, B. H., and Smith, R. T., 2015. "Low-Profile Jamming Technology for Medical Rehabilitation". *IT Prof.*, 17(5), Sept., pp. 28–34.
- [18] Hadi Sadati, S. M., Noh, Y., Elnaz Naghibi, S., Kaspar, A., and Nanayakkara, T., 2015. "Stiffness Control of Soft Robotic Manipulator for Minimally Invasive Surgery (MIS) Using Scale Jamming". In *Intelligent Robotics and Applications*, H. Liu, N. Kubota, X. Zhu, R. Dillmann, and D. Zhou, eds., Vol. 9246. Springer International Publishing, Cham, pp. 141–151.
- [19] Tognarelli, S., Brancadoro, M., Dolosor, V., and Menciassi, A., 2018. "Soft Tool for Gallbladder Retraction in Minimally Invasive Surgery Based on Layer Jamming". In 2018 7th IEEE International Conference on Biomedical Robotics and Biomechatronics (Biorob), IEEE, pp. 67– 72.
- [20] Amanov, E., Nguyen, T.-D., Markmann, S., Imkamp, F., and Burgner-Kahrs, J., 2018. "Toward a Flexible Variable Stiffness Endoport for Single-Site Partial Nephrectomy". *Annals of Biomedical Engineering*, 46(10), Oct., pp. 1498–1510.
- [21] Choi, W. H., Kim, S., Lee, D., and Shin, D., 2019. "Soft, Multi-DoF, Variable Stiffness Mechanism Using Layer Jamming for Wearable Robots". *IEEE Robot. Autom. Lett.*, 4(3), July, pp. 2539–2546.
- [22] Chen, R., Wu, L., Sun, Y., Chen, J.-Q., and Guo, J.-L., 2020. "Variable stiffness soft pneumatic grippers augmented with active vacuum adhesion". Smart Mater. Struct., 29(10), Oct., p. 105028.
- [23] Choi, I., Corson, N., Peiros, L., Hawkes, E. W., Keller, S., and Follmer, S., 2018. "A Soft, Controllable, High Force Density Linear Brake Utilizing Layer Jamming". *IEEE Robotics and Automation Letters*, 3(1), Jan., pp. 450–457.
- [24] Zhang, Y., Wang, D., Wang, Z., Zhang, Y., and Xiao, J., 2019. "Passive Force-Feedback Gloves With Joint-Based Variable Impedance Using Layer Jamming". *IEEE Trans. Haptics*, 12(3), July, pp. 269–280.
- [25] Acevedo, R., Santos, L., Pedersen, R. D., Goyal, N., Bruck, N. M., Gupta, S. K., and Bruck, H. A., 2020. "Characterization and Modeling of Layer Jamming for Designing Engineering Materials with Programmable Elastic-Plastic Behavior". *Exp Mech*, 60(9), Nov., pp. 1187–1203.
- [26] Narang, Y. S., Vlassak, J. J., and Howe, R. D., 2018. "Mechanically Versatile Soft Machines through Laminar Jamming". Advanced Functional Materials, 28(17), Apr., p. 1707136.
- [27] Zeng, X., Hurd, C., Su, H.-J., Song, S., and Wang, J., 2020. "A parallel-guided compliant mechanism with variable stiffness based

- on layer jamming". *Mechanism and Machine Theory*, **148**, June, p. 103791.
- [28] School of Mechanical Engineering, Ariel University, Israel, and Tenne, Y., 2019. "Enhancing Simulation-Driven Optimization by Machine-Learning". *IJMO*, Aug., pp. 230–233.